ACS SENSORS

Article

Cite This: ACS Sens. 2019, 4, 2706−2715

pubs.acs.org/acssensors

On-the-Spot Detection and Speciation of Cannabinoids Using Organic Thin-Film Transistors

Zachary J. Comeau,[†,‡] Nicholas T. Boileau,[‡] Tiah Lee,[§] Owen A. Melville,[‡] Nicole A. Rice,[‡] Yen Troung,[†] Cory S. Harris,[§] Benoît H. Lessard,*[,‡] and Adam J. Shuhendler*[,†,§,∥]

[†]Chemistry & Biomolecular Sciences, [‡]Chemical & Biological Engineering, and [§]Biology, University of Ottawa, Ottawa, Ontario K1N 6N5, Canada

[∥]University of Ottawa Heart Institute, Ottawa, Ontario K1Y 4W7, Canada

Supporting Information

ABSTRACT: Quality control is imperative for *Cannabis* since the primary cannabinoids, Δ^9-tetrahydrocannabinol (THC) and cannabidiol (CBD), elicit very different pharmacological effects. THC/CBD ratios are currently determined by techniques not readily accessible by consumers or dispensaries and which are impractical for use in the field by law-enforcement agencies. CuPc- and F_{16}-CuPc-based organic thin-film transistors have been combined with a cannabinoid-sensitive chromophore for the detection and differentiation of THC and CBD. The combined use of these well-characterized and inexpensive p- and n-type materials afforded the determination of the CBD/THC ratio from rapid plant extracts, with results indistinguishable from high-pressure liquid chromatography. Analysis of the prepyrolyzed sample accurately predicted postpyrolysis THC/CBD, which ultimately influences the psychotropic and medicinal effects of the specific plant. The devices were also capable of vapor-phase sensing, producing a unique electrical output for THC and CBD relative to other potentially interfering vaporized organic products. The analysis of complex medicinal plant extracts and vapors, normally reserved for advanced analytical infrastructure, can be achieved with ease, at low cost, and on the spot, using organic thin-film transistors.

KEYWORDS: *analytical methods, CBD, organic thin-film transistors, sensors, THC*

Since 2012, there has been a growing international trend toward the legalization of *Cannabis* for recreational and/or medicinal use, in some cases with limitations, restrictions, and government control, in over 40 countries worldwide, with others in the process of legalization.[1−4] While the plant, *Cannabis sativa*, is also used for fiber and seed/oil (hemp), the drug-like properties are generally associated with the inflorescence, which contains a variety of unique cannabinoids,[5] often in high concentrations. Cannabinoids are produced by the plant as carboxylic acids that can be decarboxylated into their more pharmacologically active homologs by exposure to heat, light, or prolonged storage.[6] Among over 100 identified cannabinoids,[7,8] Δ^9-tetrahydrocannabinol (THC) and cannabidiol (CBD), the decarboxylated forms of Δ^9-tetrahydrocannabinolic acid (THCa) and cannabidiolic acid (CBDa) are the most abundant and, due to their psychoactive and therapeutic effects, the most sought after by consumers (Figure 1a). The psychogenic effects of THC may be attributed to the engagement of cannabinoid receptor 1 (CB_1), making it recreationally useful, but challenging as a therapeutic agent.[9] CBD is nonpsychoactive and has a very low affinity for cannabinoid receptors but provides a variety of clinically validated and experimental indications for therapeutic use.[10−13] Therefore, THC and CBD content labeling of *Cannabis* and related products is mandatory in Canada as it is in the best interest of consumers, industry, and regulators alike, for reasons of safety and efficacy as well as quality control and law enforcement.

Currently, the most common and accurate methods of measuring cannabinoids employ high-pressure liquid or gas chromatography (HPLC or GC); however, for many companies and most consumers with limited resources and expertise, these instruments are not an accessible option. Fee-for-service cannabinoid testing is increasingly available but expensive and results may be delayed by shipping or backlogs. Law-enforcement officials have similarly struggled with establishing a definitive analytical field method to detect *Cannabis* and *Cannabis* impairment.[14−17] Recently, smaller GC and Fourier-transform near-infrared technologies have been developed as alternatives but there is a present and growing need for rapid, on-the-spot, and low-cost differentiation of cannabinoids.

Small molecules have been reported for cannabinoid detection, the majority of which are chromogenic in nature. Fast blue BB (4-amino-2,5-diethoxybenzanilide diazotated zinc double salt, or FBBB) has emerged as the most well-characterized molecular sensor, undergoing covalent modifica-

Received: June 22, 2019
Accepted: August 14, 2019
Published: August 27, 2019

DOI: 10.1021/acssensors.9b01150
ACS Sens. 2019, 4, 2706−2715

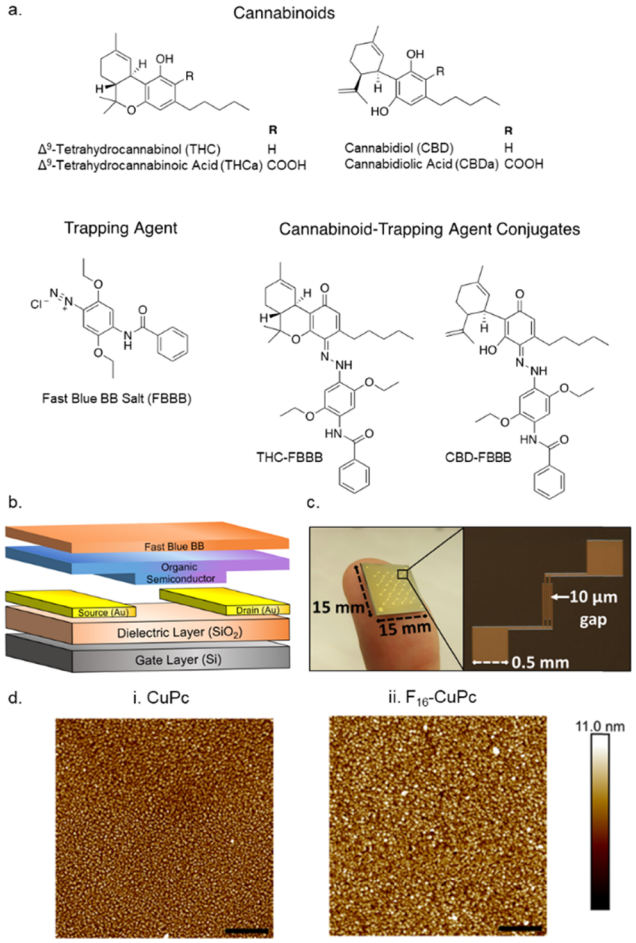

Figure 1. (a) Molecular structures of primary cannabinoids, trapping agent (FBBB), and cannabinoid-trapping agent conjugates. (b) Electronic device architecture cross section. (c) Image of a Fraunhofer IPMS chip and enlarged brightfield microscopy image of a single bottom-gate bottom-contact (BGBC) device substrate with a 10 μm channel width. (d) Atomic force microscopy (AFM) images of (i) CuPc and (ii) F_{16}-CuPc substrates. Black scale bars represent 500 nm.

tion by cannabinoids under alkaline conditions to afford a rapid colorimetric test to detect THC (Figures 1a and S1),[18−20] which is still in use by law-enforcement agencies.[20] While the very high limit of detection and rapid rate of reaction of FBBB with cannabinoids is ideally suited as a cursory sampling tool, critically, the method in its optical form is limited by its lack of specificity.[21−23] However, the color change that occurs upon the reaction of FBBB with cannabinoids suggests alterations in band-gap energies between free FBBB and the FBBB−cannabinoid complex, which, we hypothesize, will translate to differential modulation of charge transport with the layering of an alkaline FBBB-based thin film onto organic thin-film transistors (OTFTs).

OTFTs have shown promise as low-cost, disposable, and mechanically robust sensors.[24] They are operated by applying a fixed source-drain voltage (V_{SD}) across an organic semiconductor (OSC) while modulating the current that flows through it (I_{SD}) with bias from an insulated gate electrode (V_{GS}) (Figure 1b,c). OSC materials can transport either holes (p-type) or electrons (n-type) at a rate quantified by the field-effect mobility, μ_H or μ_E, respectively, which increases sharply when V_{GS} exceeds the threshold voltage (V_T) and continues to vary as a function of V_{GS}.[25,26] Molecular structure, frontier orbital energies, film crystallinity, device engineering, and characterization environment all have been shown to affect OTFT performance, including both μ and V_T.[25,27,28] In addition, changes in these sensitive electrical properties can be measured in response to the introduction of interactive chemical species. To date, OTFTs have been developed for the detection of a variety of medically relevant fluid-based analytes[29−34] and environmental gases,[35−37] with selectivity being attained by assembling multiple sensors into an array. However, the application of OTFTs for the detection and/or differentiation of *Cannabis* components from crude plant extracts or vapor-phase plant samples is unprecedented.

In this study, we demonstrate the rapid sensing of cannabinoids in FBBB-sensitized OTFTs and evaluate the hypothesis that the energy changes of FBBB upon analyte binding are responsible for significant OTFT performance variations that could yield practical analytical capabilities. p-type copper phthalocyanine (CuPc) and n-type copper hexadecafluorophthalocyanine (F_{16}-CuPc) were selected as the OSCs for these devices as they are air-stable, well characterized, and inexpensive materials with different energetics and majority charge carriers that might differentiate their sensing responses to cannabinoid analytes. We examine the effects these primary cannabinoids have on device performance and use these results to develop a method for determining the primary cannabinoid ratio in unprocessed liquid extracts of plant material with accuracy indistinguishable to that obtained by HPLC analysis. We also apply our devices to sensing vaporized cannabinoids and demonstrate a method for their selective detection. Finally, we investigate the mechanisms for cannabinoid detection in FBBB-integrated OTFT devices by solid-state UV−vis spectroscopy. The current work establishes the potential utility of OTFTs for expeditious, low-cost, on-the-spot quality control assessment for the *Cannabis* producer and consumer, as well as for law enforcement and border protection services. More broadly, this work demonstrates the utility of integrating chromogenic substrates into OTFTs with the potential to enhance analyte sensitivity, sensor portability, and analytical selectivity.

RESULTS AND DISCUSSION

Device Architecture and Detection of Cannabinoids.

Bottom-gate bottom-contact (BGBC) OTFTs were fabricated by the physical vapor deposition of 150 Å semiconducting films of either CuPc or F_{16}-CuPc on octyltrichlorosilane (OTS)-treated Si/SiO_2 substrates with prepatterned gold source-drain electrodes (Figure 1b,c). OTS was used as a pretreatment as it forms a self-assembled monolayer that helps promote consistent surface morphology, improving the overall device performance.[26,38] The deposited semiconductor films were confirmed to be homogenous by atomic force microscopy (AFM) with results consistent with literature values obtained under similar conditions (Figure 1di,ii).[39,40]

To sensitize the OTFTs to cannabinoid analytes, a thin film of alkaline FBBB (pH 9, NaOH as a base) in acetonitrile (ACN) was drop-cast on top of the semiconductor layer (Figure 1b). Device performance was analyzed in ambient conditions to reflect those in which *Cannabis* samples would most likely be tested. Due to small variations in the baseline device performance, the calculated peak baseline mobility (eq 2) of each device was linearly scaled to the overall average. Application of this vertical scaling factor yielded the adjusted mobility that facilitates direct comparison between devices

DOI: 10.1021/acssensors.9b01150
ACS Sens. 2019, 4, 2706−2715

prior to the addition of analytes. After the addition of a thin film of alkaline FBBB (20 μM, FBBB(B)) to these baseline CuPc and F_{16}-CuPc devices, the maximum current observed in their respective output curves does not change substantially (Figure 2ai-ii,bi-ii). However, the subsequent addition of an analytical standard THC (20 μM, plant extract concentrate, 97% purity) solution directly onto the OTFT surface caused a substantial reduction in the maximum current, roughly 20- and 2-fold for CuPc- and F_{16}-CuPc-based devices, respectively (Figure 2aiii,biii). In addition to a decrease in the maximum current, the application of analytical standards of either THC or CBD (plant extract concentrate, 99% purity) to the FBBB-sensitized devices resulted in a large negative V_T shift, particularly for F_{16}-CuPc, that can be observed as shifts to the left in their transfer curves (Figure 2c,d). Overall, these significant changes in OTFT I_{SD} and V_T are indicative of altered charge transport properties caused by the addition of liquid samples of THC or CBD onto the device surface.

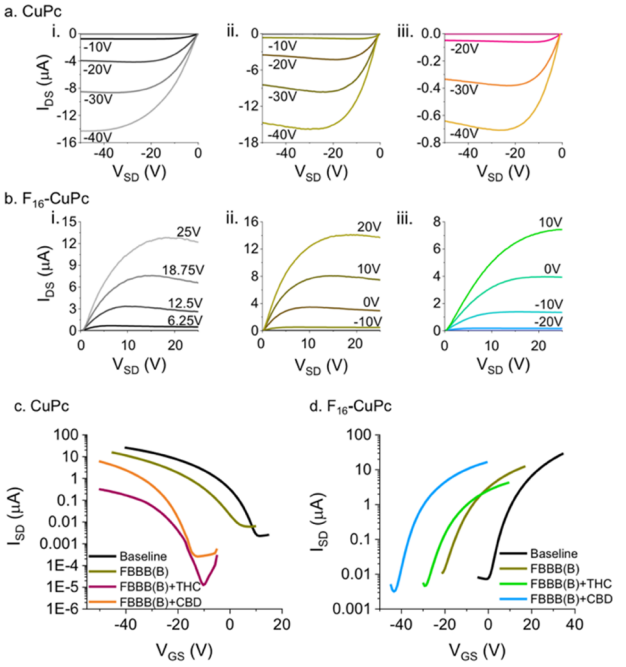

Figure 2. Sample output and transfer curves of OTFT devices. Output curves obtained for characteristic (a) CuPc and (b) F_{16}-CuPc devices for (i) a semiconductor-only device, (ii) following the application of 20 μM FBBB with 50 μM NaOH in ACN (FBBB(B)), and (iii) following FBBB(B) deposition and after exposure to 20 μM THC in ACN. Transfer curves, (c, d), obtained for CuPc and F_{16}-CuPc devices with various treatments (20 μM THC or CBD). Note the differences in the y-axis scales between panels.

To more thoroughly examine the observed changes in the performance upon cannabinoid addition to FBBB-sensitized devices, CuPc and F_{16}-CuPc OTFTs were characterized after exposure to different combinations of detection components, including ACN, NaOH (base), FBBB, FBBB with NaOH (FBBB(B)), and the cannabinoids themselves (THC and CBD). Repeated applications of ACN showed sequential decreases of 14.2 and 8.5% in μ_H on CuPc-based devices and 15.2 and 2.4% decreases in μ_E on devices comprising F_{16}-CuPc (Figure S2). A single addition of NaOH showed a 29.2% decrease in μ_H and an 8.0% decrease in μ_E (Figure S2). The addition of FBBB as a thin film overlying the semiconducting layer caused an approximate 46.5% decrease in μ_H on CuPc and a 59.5% decrease in μ_E on F_{16}-CuPc from the baseline, with an observed ±3 V shift in V_T (Figure 3aii,bii). The addition of alkaline FBBB (pH 9) resulted in a −11 and −15 ΔV_T, with an additional 7.1% drop in μ_H and a 10.1% drop in μ_E from FBBB on CuPc- and F_{16}-CuPc-based OTFTs, respectively (Figure 3ai,bi). THC alone, THC with NaOH, and THC with FBBB all displayed a combined average 53.0 ± 6.9% decrease in μ_H and 61.1± 2.4% decrease in μ_E from the baseline (Figure 3aiii,biii). The addition of any impurity typically causes a reduction in mobility; however, only in the presence of a thin film of alkaline FBBB did the subsequent addition of THC induce a significant decrease in both μ_H and μ_E (96.0 and 98.9%, respectively) from that observed with FBBB alone (Figure 3ai,bi). The addition of CBD (plant extract concentrate, 99% purity) to devices with alkaline FBBB resulted in a ΔV_T of roughly −20 V with an 81% decrease in μ_H and 58.1% decrease in μ_E relative to baseline (Figure 3ai,bi), distinct changes from those observed for THC.

To provide evidence that the reaction between FBBB and the phenolic center is necessary for cannabinoid sensing by OTFT, device performance after treatment with the model phenols resorcinol and 3-methoxyphenol was assessed (Figure S3). As was observed with THC and CBD, a substantial decrease in the adjusted mobility ($\Delta\mu_H$ = −76.8 and −73.9%, $\Delta\mu_E$ = −82.9 and −80.3%) and voltage threshold (CuPc ΔV_T = −5 and 0, F_{16}-CuPC ΔV_T = 0 and 10) were recorded for devices bearing alkaline FBBB when exposed to resorcinol and 3-methoxyphenol, respectively (Figure S3bii,cii). Device responses (μ and V_T) recorded were easily differentiable from those observed with THC and CBD, likely due, in part, to differences in π-conjugation and hydrophobicity of the phenols. Further support for molecular determinants of analyte detection by alkaline FBBB-bearing OTFTs was obtained by testing the device against cannabigerol (CBG), a biosynthetic intermediate to THC and CBD bearing an alkyl-substituted resorcinol moiety (Figure S3a,bi,ci). CBG produced a response more closely matching that of resorcinol than THC and CBD, with a decrease of 77.8 and 88.7% in μ_H and μ_E, respectively, and of 5 and 0 V in ΔV_T on CuPc and F_{16}-CuPc, respectively (Figure S3). While all of the components of the thin film deposited on the semiconductor have some effect on μ and V_T relative to uncoated devices, alterations in the device performance are amplified by the reaction of the phenol moiety of the analyte with the alkaline FBBB of the device. Furthermore, this reaction facilitates analyte differentiation by specific alterations of performance parameters related to the specific chemical structures of the analyte.

Determination of THC/CBD Ratios from Liquid Samples. From the μ−V_{GS} curves obtained from the transfer data, it was noted that the OTFT readouts were characteristic of the cannabinoid type applied, with THC and CBD yielding differential responses on both CuPc and F_{16}-CuPc (Figure 3ai vs bi). From this observation, we hypothesized that CuPc and F_{16}-CuPc could be used in parallel as the active materials in OTFT-based sensors for the differential detection of THC and CBD when using a thin film of alkaline FBBB as cannabinoid complexing agent. To test this hypothesis, THC and CBD mixtures comprising of analytical standard plant extract concentrates were prepared in 1:3, 1:1, and 3:1 molar ratios and were applied to the surface of devices coated with alkaline FBBB. For CuPc-based devices, the adjusted mobility varied inversely with higher THC to CBD content, with limited

DOI: 10.1021/acssensors.9b01150
ACS Sens. 2019, 4, 2706−2715

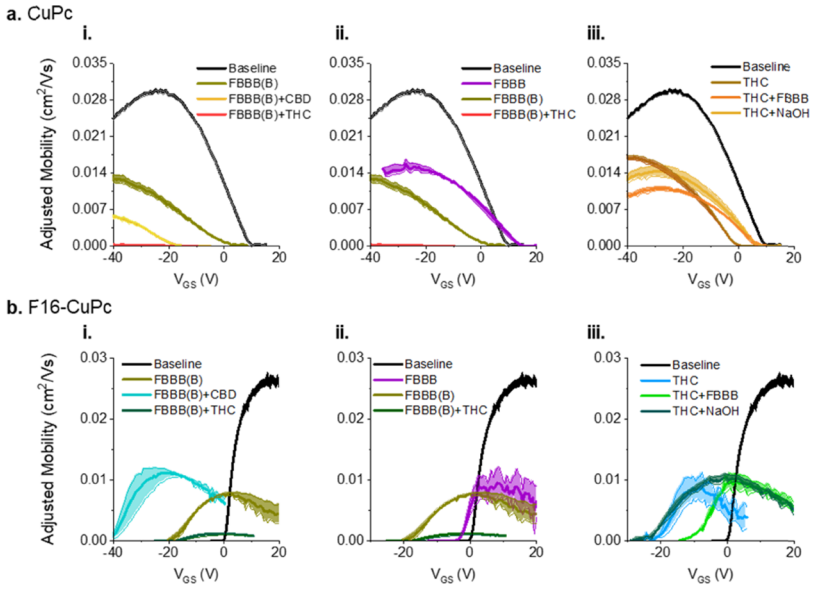

Figure 3. Effect of applied analyte on the field-effect mobility of OTFTs with respect to the applied gate-source voltage (V_{GS}). Field-effect mobility was evaluated for OTFTs consisting of (a) CuPc or (b) F_{16}-CuPC semiconductors prior to further manipulation (baseline), following 20 μM FBBB deposition (FBBB), 20 μM alkaline (pH 9) FBBB deposition (FBBB(B)), deposition of alkaline FBBB and the subsequent addition of 0.5 μL of 20 μM analytical standard solutions of THC or CBD (FBBB(B) + THC, (FBBB)B + CBD), following deposition of THC standards (THC) or alkaline THC standards (THC + NaOH). Data represent the mean (solid line) and data range (i.e., min. to max. values, shaded region) of three V_{GS} sweeps at saturation across eight devices. Mobilities were calculated between adjacent points of the transfer data.

changes in V_T of < 5 V (Figure 4ai). In contrast, for F_{16}-CuPc-based OTFTs, adjusted mobility varied inversely, and V_T varied directly with increasing THC to CBD content (Figure 4bi). These electrical differences between THC and CBD outputs could be due to variations in the molecular structure of the FBBB−cannabinoid complexes. The FBBB−THC complex is more planar in character, has increased π electron delocalization, and may better align between grain boundaries, further limiting charge transfer, while FBBB−CBD may form lower density aggregates.[27,41] Overall, the adjusted mobility maxima for each intermediate ratio (1:3, 1:1, and 3:1) were found to lie between those obtained for pure THC and CBD extract solutions, with the total device output dependent upon the relative cannabinoid content, suggesting that the alkaline FBBB-integrated OTFTs may be capable of rapid cannabinoid speciation.

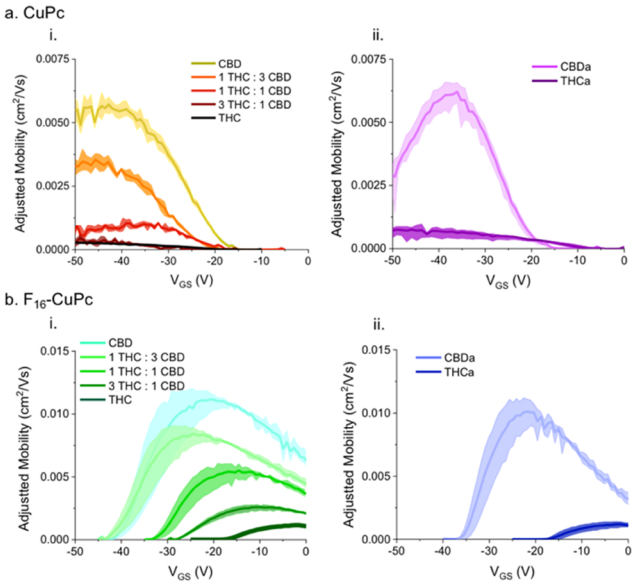

Figure 4. Effect of primary cannabinoid ratios on field-effect mobility of alkaline FBBB-treated OTFTs with respect to gate-source voltage (V_{GS}). Field-effect mobility was evaluated for OTFTs consisting of alkaline FBBB (20 μM)-treated (a) CuPc or (b) F_{16}-CuPc semiconductors following the addition of 0.5 μL of a 20 μM analytical standard in ACN of THC to CBD as a ratio (i), or pure THCa or CBDa (ii). Data represent the mean (solid line) and data range (shaded region) of three V_{GS} sweeps at saturation across eight devices. Mobilities were calculated between adjacent points of the transfer data using eq 2.

An important consideration for cannabinoid analysis is that cannabinoids from plants are effectively in a "prodrug" form, existing as cannabinolic acids that must be decarboxylated, often by pyrolysis, to their respective cannabinol form to have pharmacological effects. To evaluate the effect of these cannabidiolic acids on the device performance, analytical standard solutions of THCa and CBDa were applied to the OTFTs. The corresponding mobility curves were found to approximate those of pure THC and CBD, respectively (CuPc: THC/THCa $\Delta\mu = -4.5 \times 10^{-4}$ cm^2/(V s), $\Delta V_T = 6$ V, CBD/CBDa $\Delta\mu = -4.0 \times 10^{-5}$ cm^2/(V s), $\Delta V_T = -1$ V; F_{16}-CuPc: THC/THCa $\Delta\mu = -4.9 \times 10^{-5}$ cm^2/(V s), $\Delta V_T = -2$ V, CBD/CBDa $\Delta\mu = 1.0 \times 10^{-3}$ cm^2/(V s), $\Delta V_T = 7$ V) (Figure 4aii,bii). While pharmacologically distinct from the decarboxylated cannabinoid compounds, our results show that, through extract analysis via OTFT, the cannabinolic acid is undifferentiable from the respective cannabinol form. Since heating (i.e., baking or smoking) induces decarboxylation,[6] we hypothesize that the total complement of (THC + THCa)/(CBD + CBDa) in a sample prepyrolysis can be determined by alkaline FBBB-coated OTFTs and furthermore can predict postpyrolysis THC/CBD content.

To test this hypothesis and apply the alkaline FBBB-coated OTFT to the analysis of real-world *Cannabis* plants, small

DOI: 10.1021/acssensors.9b01150
ACS Sens. 2019, 4, 2706−2715

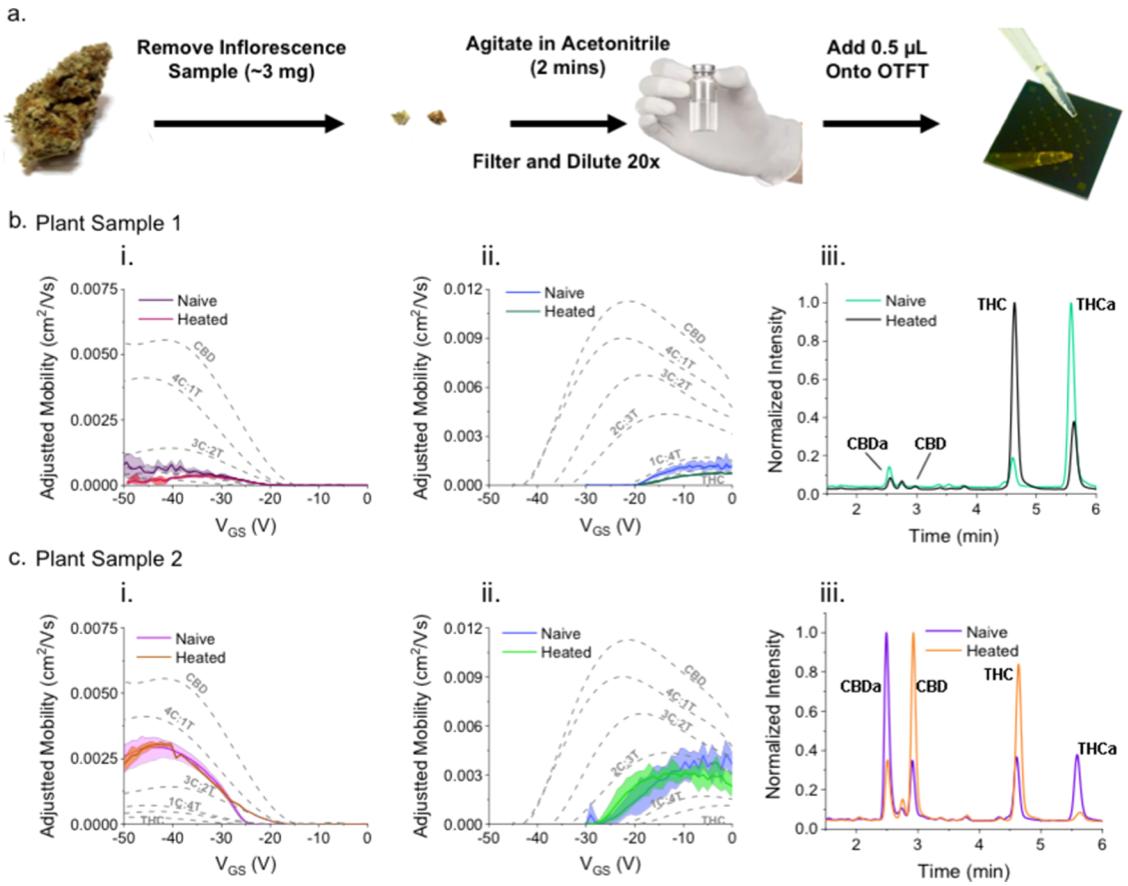

Figure 5. Estimating primary cannabinoid ratios by OTFT mobility from simple plant sample extractions. (a) Extraction workflow. (b, c) Samples of *Cannabis* inflorescence were ground, and 1 mg/mL was agitated for 2 min in ACN before microfiltration and 20× dilution. Heated samples were baked at 115 °C for 45 min. Filtered extract (0.5 μL) was applied to the surface of alkaline FBBB-treated (bi, ci) CuPc and (bii, cii) F16-CuPc OTFTs and the field-effect mobility was linearly compared (Table 1) to linear fit fifth-order polynomial standard curves obtained from the analytical standard cannabinoid ratios (Figure 4a). Data represent the mean (solid line) and data range (shaded region) of three V_{GS} sweeps at saturation across eight devices. (biii, ciii) HPLC-DAD analysis was performed on 2 μL of filtered extract prior to dilution. Samples were eluted at 0.25 mL/min in 50−100% H_2O/ACN with 0.1% FA at 65 °C. Chromatograms were detected at 210 nm and intensity-normalized. HPLC ratios were determined by areas under the curve.

samples (~3 mg) were harvested from the inflorescence of two different plants, both confirmed by the supplier to contain approximately 20% w/v primary cannabinoids (Hydropothecary). A simple extraction on the naïve *Cannabis* bud samples was carried out where approximately 3 mg of the plant material in ACN (1 mg/mL) was manually agitated for 2 min, filtered, and diluted 20-fold in ACN prior to addition directly to the device surface (Figure 5a). The dilution step was necessary to avoid overloading the devices, which were found to have a sensitivity range below 1.5 pg to a maximum of 3.15 ng of cannabinoid (Figure S4). Concentrations greater than 3.15 ng of THC resulted in no field effect being observed, and concentrations at 1.58 pg had a minimal effect (<5%) relative to that already observed from the alkaline FBBB treatment. Longer and mechanically agitated extractions of plant material in ACN or 80:20 MeOH/H_2O, a gold standard solvent for extraction of bioactive compounds from plants,[42] did not improve the 90−95% extraction efficiency obtained by short manual agitation (Figure S5). A portion of the obtained plant extract was heated at 115 °C for 45 min to decarboxylate cannabinolic acids to their cannabinol form,[43] while another portion was left unheated. HPLC analysis of these extracts confirmed that 73 and 85 wt% of samples 1 and 2, respectively, were decarboxylated (Figure 5biii,ciii). Peak identities were confirmed by comparing retention times against those resulting from authentic cannabinoid standard samples (Figure S6). Mobility curves were obtained after applying a drop (approximately 0.5 μL) of plant extracts with and without pyrolysis treatment directly onto CuPc and F_{16}-CuPc devices (Figure 5a), and the ratio of THC to CBD was determined by linear interpolation of the average $\mu-V_{GS}$ curve for each *Cannabis* plant sample extract between the standard curves generated from analytically pure THC/CBD solutions (Figure 5bi-ii,ci-ii, dashed lines, and Table 1).

CuPc-based devices consistently predicted ratios slightly greater than those determined by HPLC for each plant sample, while F_{16}-CuPc-based devices consistently predicted smaller values. The THC/CBD ratio determined by averaging CuPc- and F_{16}-CuPc-based analyses resulted in an error rate of 5.5%, matching the accuracy of ratios determined by HPLC that fall within 3−10% of the real value due to extraction inefficiencies, variations in inflorescence composition, and varying maximal absorbances of the primary cannabinoids assayed.[44,45] These results suggest that CuPc- and F_{16}-CuPc-based OTFTs can be used to identify the ratio of THC to CBD following simple *Cannabis* plant extractions and that the analysis of preheated samples (i.e., majority cannabinoids in an acid form) predict THC and CBD content postpyrolysis (i.e., in the decarboxy-

DOI: 10.1021/acssensors.9b01150
ACS Sens. 2019, 4, 2706−2715

Table 1. Comparison of Estimates by OTFT of Primary Cannabinoid Ratios to HPLC-DAD from Simple Plant Sample Extractions[a]

	measured cannabinoid ratio (CBD/THC)	
measurement method	plant sample 1	plant sample 2
CuPC	11:89 ± 4.5	66:34 ± 0.7
F_{16}-CuPC	5:95 ± 0.5	36:64 ± 0.4
OTFT average	8:92	51:49
HPLC	3:97	57:43

[a]Mobilities from −40 to −50 V_{GS} for CuPc and −10 to 0 V_{GS} for F_{16}-CuPc OTFTs were linearly fit to fifth-order polynomial standard curves and averaged for each plant sample. Standard deviation is also shown. Ratios for each material were averaged again to give the OTFT average. HPLC ratios were determined by direct comparison of peak areas.

lated and medicinally/recreationally efficacious bioactive form).

Detection of Vaporized Cannabinoids. While on-the-spot plant extract analysis is of interest to producers, dispensaries, and consumers, cannabinoid detection from the vapor phase is of special interest to law enforcement seeking objective measures of *Cannabis* use in prohibited environments (e.g., automobiles). To this end, alkaline FBBB thin-film-bearing OTFT devices were exposed to THC or CBD vapor, as well as a variety of vaporized materials that were previously indicated to interfere with FBBB-mediated cannabinoid detection (coffee grounds or wood smoke),[18] or that might be found alongside *Cannabis* (cigarette or e-cigarette smoke). Following 1.5 min exposure to equivalent vapor volumes, μ–V_{GS} curves for the CuPc- and F_{16}-CuPc-based OTFTs were obtained (Figure 6a,b). Exposure to THC vapor (3.125 mg/L) resulted in a substantially reduced μ_H and μ_E on both CuPc- and F_{16}-CuPc-based devices and a $-\Delta V_T$ of 35 V on F_{16}-CuPc (Figure 6). Devices exposed to CBD vapor (3.125 mg/L) behaved similarly to those exposed to liquid samples, with a decrease in μ_H and μ_E on both CuPc- and F_{16}-CuPc-based devices, with a $-\Delta V_T$ of 18 V on F_{16}-CuPc. This greater $-\Delta V_T$ shift on F_{16}-CuPc-based devices when exposed to THC, compared to those exposed to CBD, could be due to noncomplexed THC and CBD interacting with the devices, with the former found to cause a deeper $-V_T$ shift on its own (Figure S7). In an effort to understand the interactions of the alkaline FBBB-coated OTFT devices with cannabinoids that result in the observed detection and speciation capabilities, solid-state absorbance spectroscopy was performed. Absorbance spectra show decreasing Q-band intensities in CuPc when treated with alkaline FBBB, with a further decrease when subsequently exposed to THC vapor (Figure S8). Such Q-band intensity reduction is characteristic of an interruption in π–π^* interactions, supporting the observed loss of hole-transport capability of CuPc upon the formation of the FBBB–THC complex.[46,47] For F_{16}-CuPc, only a minimal decrease in the Q-band absorbance is observed, possibly due to the protective nature of the axial fluorines. A slight increase in the Soret band points to electron doping and interactions with the central copper, expected due to the large $-\Delta V_T$ shifts observed.[46,47] Our research group has found that F_{16}-CuPc-based OTFTs are more susceptible to large V_T shifts relative to CuPc-based OTFTs when exposed to an analyte.[31] With a larger observed grain size and smoother surface (Figure 1), the variations in response of F_{16}-CuPc versus CuPc OTFTs may

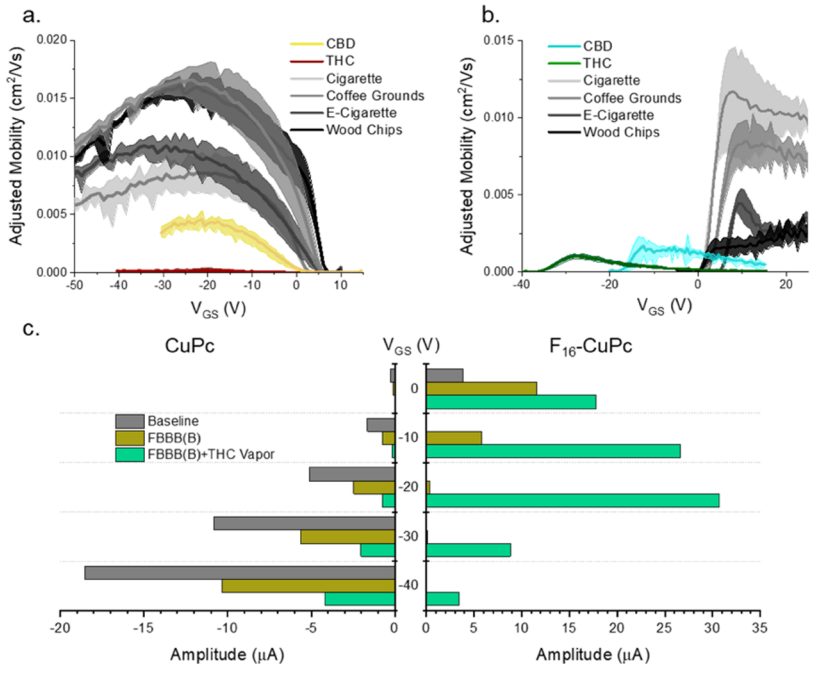

Figure 6. Effects of vapor treatments and single current output on field-effect OTFTs with respect to gate-source voltage (V_{GS}). Field-effect mobility was evaluated for OTFTs consisted of alkaline FBBB (20 μM)-coated (a) CuPc or (b) F_{16}-CuPc semiconductors following exposure to vaporized THC, CBD, cigarette, coffee grounds, e-cigarette solution, or wood chips. The analyte (25 mg) was completely vaporized at 210 °C into an 8 L bag and allowed to flow over the devices for 90 s. Data represent the mean (solid line) and data range (shaded region) of three V_{GS} sweeps at saturation across eight devices. Mobilities were calculated between adjacent points of the transfer data. (c) Gate-source (V_{GS}) and source-drain (−50 V for CuPc (left) and 25 V for F_{16}-CuPc (right)) voltages were held constant and the current was measured over 10 s and averaged. Bars represent the average of 10 readings; minimum and maximum current is <0.017 μA from the average and are not visible on the plot.

DOI: 10.1021/acssensors.9b01150
ACS Sens. 2019, 4, 2706−2715

also be partially explained by morphological differences between the films.

Interfering vapor compounds (e-cigarette smoke, wood smoke, and burnt coffee grounds) were evaluated for their effects on alterations in device performance for both CuPc and F_{16}-CuPc OTFTs. e-Cigarette smoke caused the greatest $+\Delta V_T$ shift, likely due to its high concentration of propylene glycol,[48] which contains many electron-trapping hydroxyl groups (Figure 6a). Wood smoke and burnt coffee grounds, despite being high in phenolic compounds and interacting with alkaline FBBB in liquid,[18] may have done so in a limited fashion in the vapor phase, resulting in smaller property changes (Figure 6b). For CuPc-based devices (μ_H), the mobility reduction caused by the cannabinoids was substantially greater (10- and 2-fold for THC and CBD, respectively) than any of the interfering compounds. Similarly, interfering vapors were readily differentiable from CBD and THC vapor by their effects on V_T on F_{16}-CuPc-based devices. Only THC and CBD resulted in ΔV_T <0 V, with $V_T^{THC} = -35$ V and $V_T^{CBD} = -23$ V (Figure 6b).

Due to the specific response of both types of OTFT, elicited at $V_{GS} < 0$ V when exposed to vapor-phase THC compared to other interfering compounds, a simple device implementation scheme for vapor-phase THC detection was tested. Rather than capturing the full range of electrical data in a $\mu-V_{GS}$ curve and compared to standards, the signal output (I_{SD}) of the devices was measured before and after the THC vapor exposure at specific electrical inputs (Figure 6c). CuPc-based devices sensitized with an alkaline FBBB layer showed the highest change in signal when $V_{GS} = -20$ V, with a 5-fold decrease in the current after THC exposure. On the other hand, F_{16}-CuPc-based alkaline FBBB-coated devices demonstrated a maximum 30-fold increase in I_{DS} at $V_{GS} = -20$ V after exposure. This turn-on response is generally desirable for sensing as changes that cause increases in the current are harder to cause incidentally and easier to detect.[49] When combined, a CuPc- and F_{16}-CuPc-based device array with $V_{GS} = -20$ V could detect both changes in the current for a more sensitive or specific detection of THC. Although the applied biases may seem high, fine-tuning the device architecture and dimensions could reduce them to more reasonable levels for practical use. Overall, CuPc- and F_{16}-CuPc-based devices produced an electrical fingerprint that uniquely identified cannabinoids over other interfering compounds in the vapor phase, with the potential to detect and speciate CBD from THC when analyzing both extrinsic semiconductors in an array.

CONCLUSIONS

Herein, we present an OTFT-based sensor consisting of two well-known organic semiconducting materials, CuPc and F_{16}-CuPc, coated with an alkaline FBBB-based thin film for the specific detection and speciation of the major cannabinoid components of the *Cannabis* plant. Detection and speciation were demonstrated for the direct analysis of simple liquid (Figure 5) and vapor-phase samples (Figure 6). The overlying thin film of alkaline FBBB on top of the semiconductor layer was found to be necessary to induce a substantial decrease in the charge transport mobility and threshold voltage on both semiconducting materials upon exposure to cannabinoids (Figures 2 and 3). The ratio of decarboxylated cannabinoids in the postpyrolyzed product was accurately predicted following a simple, manual plant extract procedure to within 5.5% of the CBD/THC obtained by HPLC analysis when averaged between CuPc and F_{16}-CuPc. Therefore, the postpyrolysis ratio of pharmacologically active THC and CBD can be predicted through the analysis of prepyrolyzed plant sample extract. Furthermore, the presence of THC vapor was readily detected through simple changes in the OTFT output current, with F_{16}-CuPc devices showing a significant turn-on response when operating in reverse bias. Potentially interfering vapor compounds did not induce comparable changes to electrical properties relative to that of THC or CBD. This could be useful for the specific, rapid detection of vaporized THC in applications such as law enforcement.

The OTFT devices described herein afford on-the-spot cannabinoid analysis that is unprecedented among existing analytical techniques: compact, low cost, simple sample preparation, rapid analysis, and capable of liquid- or vapor-phase detection and speciation of THC and CBD, the main cannabinoids of interest for recreational and medicinal use, respectively. This work initiates the application of OTFT technologies for cannabinoid sensing upon which engineering of device architecture and the synthesis of new cannabinoid-sensitive materials could improve specificity and sensitivity, opening the door to full cannabinoid quantitation. In addition, the integration of the analyte-sensitive chromophores into the OTFT was shown to extend device-based sensing to complex, real-world samples and helps to lay the groundwork for expanding OTFT-based sensing through reactive chromophore integration.

MATERIALS AND METHODS

Materials. All chemicals were used as received unless otherwise specified. Copper phthalocyanine (CuPc, 90%) and copper(II) 1,2,3,4,8,9,10,11,15,16,17,18,22,23,24,25-hexadecafluoro-29*H*,31*H*-phthalocyanine (F_{16}-CuPc, >99.9%) were obtained from TCI Chemicals. CuPc was purified twice by train sublimation before use. 4-Amino-2,5-diethoxybenzanilide diazotated zinc double salt (Fast Blue BB, FBBB), (octyl)trichlorosilane (OTS, 97%), resorcinol, and 3-methoxyphenol were obtained from Sigma-Aldrich. All solvents were HPLC grade and purchased from Fisher Scientific. *Cannabis* plant samples were supplied by Hydropothecary and cannabinoid standards were obtained from Toronto Research Chemicals.

Preparation of Devices. Prepatterned silicon substrates with a thermally grown, 230-nm-thick SiO_2 dielectric, and gold source-drain electrodes (W = 2000 μm, L = 10 μm) were purchased from Fraunhofer IPMS and used to make bottom-gate bottom-contact transistors. Each Fraunhofer contained four devices. Substrates were washed with acetone to remove the protective resist, rinsed with isopropanol, and dried with nitrogen, before oxygen plasma treatment for 15 min. Substrates were then washed with water, rinsed with isopropanol, and dried with nitrogen before being submerged in a solution of 0.1% v/v OTS in toluene for 1 h at 70 °C. The silane-treated substrates were then washed with toluene, rinsed with isopropanol, and dried with nitrogen. The substrates were further dried under vacuum at 70 °C for 1 h. Dried substrates were transferred into an Angstrom EvoVac thermal evaporator and 150 Å of CuPc or F_{16}-CuPc was deposited at 25 °C and pressure below 2×10^{-6} torr at a rate of 0.3 Å/s by sublimation onto respective substrates. Devices were kept under nitrogen for up to 2 days prior to characterization.

Device Characterization. The source-drain electrodes were contacted with BeCu alloy probe tips, and electrical measurements were taken using a custom electrical probe station, oesProbe A10000-P290 (Element Instrumentation Inc. & Kreus Design Inc.) with a Keithley 2614B to set discrete V_{DS} and V_{GS} values, measuring I_{DS}. From these measurements, the saturation field-effect mobility, threshold voltage, and on/off current ratio were determined. The

DOI: 10.1021/acssensors.9b01150
ACS Sens. 2019, 4, 2706−2715

general expression relating current to field-effect mobility and gate voltage in the saturation region is as follows

$$I_{DS} = \frac{\mu C_i W}{2L}(V_{GS} - V_T)^2 \quad (1)$$

where I_{DS} is the source-drain current, μ is the field-effect mobility, C_i is the capacitance, W is the width of the channel, L is the length of the channel, V_{GS} is the gate-source voltage, and V_T is the threshold voltage. Equation 1 can be rearranged, giving eq 2, such that the mobility and threshold voltage can be calculated directly from the slope and x-intercept of the $\sqrt{I_{DS}}$ vs V_{GS} curve

$$\sqrt{I_{DS}} = \sqrt{\frac{\mu C_i W}{2L}}(V_{GS} - V_T) \quad (2)$$

Baseline mobility values were obtained for each device prior to adding analytes and averaged. The maximum baseline value for the individual device was linearly scaled to the average maximum baseline value, and this scaling factor was applied to the resulting analyte mobility curves for that device. Liquid analytes, dissolved in ACN, were pipetted directly onto the source-drain channel and allowed to dry for 3 min before device characterization. Maximum and minimum obtained mobilities are displayed in plots in lieu of standard deviation to better represent reproducibility in the device performance.

Vapor Experiments. Samples were vaporized at 210 °C in a Volcano Medic Vaporizer by PharmaSystems in an 8 L bag. The vapor was allowed to cool for 1 min before being flowed over devices in a 500 mL container at an approximate rate of 90 mL/s. Wood chips were fine shavings of eastern white pine, cigarettes were Pall Mall Blue, e-cigarette fluid was Vapor Papi Original, and coffee grounds were President's Choice West Coast Dark Roast.

HPLC Analysis. Cannabinoid standards of CBD, CBDa, THC, and THCa were made to 1 mg/mL in methanol. Ground *Cannabis* plant material was extracted with 1 mg/mL of either ACN or 80:20 MeOH/H_2O and 1 mL of supernatant was filtered with a 0.22 μm PTFE syringe filter (Chromatographic Specialties Inc.) after 2, 15, 30, or 60 min of agitation in a solvent. Extracts (2 μL) were analyzed using a HPLC system (Agilent 1100 HPLC) with an inline photodiode array detector (series G1315). A polar C18 Phenomenex Luna Omega column (100 × 2.1 mm^2; particle size 1.6 μm; pore size 100 Å) was used for separation. The mobile phase consisted of water + 0.1% formic acid (mobile phase A) and ACN + 0.1% formic acid (mobile phase B). The gradient elution was the following: 0.0−1.0 min 75% B, 2.0−6.0 min 75−85% B, 6.0−7.0 min 85% B, 7.0−15.0 min 75% B, followed by a 5 min column equilibration after each run. The flow rate was set at 0.25 mL/min and the column temperature was maintained at 65 °C. The chromatograms were detected at 210 nm.

Thin-Film Characterization. UV−vis spectra were acquired on a Cary 100 spectrophotometer in a 3500 μL cuvette with a 10 mm path length (Thorlabs). Solutions of FBBB (0.1%) and FBBB (0.1%) with THC (40 μg/mL) and NaOH (0.15 M) were prepared in ACN.

AFM. Tapping mode atomic force microscopy images were obtained using a Bruker Dimension Icon AFM equipped with ScanAsyst-Air tips. Scans were performed at a scan rate of 1 Hz, with multiple locations on each surface investigated. Images were processed using NanoScope Analysis v.1.8.

Statistics. Data were analyzed by a binomial test using Prism (v.8.0.1., GraphPad Inc.).

■ ASSOCIATED CONTENT

Supporting Information

The Supporting Information is available free of charge on the ACS Publications website at DOI: 10.1021/acssensors.9b01150.

Absorbance spectra, AFM images, device data, and HPLC characterization (PDF)

■ AUTHOR INFORMATION

Corresponding Authors

*E-mail: benoit.lessard@uottawa.ca (B.H.L.).
*E-mail: adam.shuhendler@uottawa.ca (A.J.S.).

ORCID

Nicole A. Rice: 0000-0002-6442-5249
Benoît H. Lessard: 0000-0002-9863-7039
Adam J. Shuhendler: 0000-0001-6952-5217

Author Contributions

A.J.S, B.H.L, and C.S.H. conceived this project, and Z.J.C, N.T.B., O.A.M., B.H.L, and A.J.S. designed the experiments. Z.J.C. and T.L. performed HPLC analysis on extracts and performed vapor-phase testing. Y.T. synthesized and characterized cannabinoid−FBBB standards. N.A.R. captured AFM images. Z.J.C. captured UV−vis spectra, performed CV experiments, and built and characterized OTFT devices. All authors discussed the results and edited the manuscript. Z.J.C, C.S.H., B.H.L, and A.J.S co-wrote the manuscript.

Funding

This work was supported by NSERC Discovery Grant RGPIN 2015-05796 (A.J.S.) and 2015-03987 (B.H.L), the Canada Research Chairs Program 950-230754 (A.J.S.) and 950-230724 (B.H.L). We are also thankful for the following fellowships: Ontario Graduate Scholarship (OGS) to O.A.M. and the NSERC PDF to N.A.R. Infrastructure used to complete this work was acquired using CFI-JELF #30488 (B.H.L). and NSERC RTI 472921-2015 (B.H.L).

Notes

The authors declare no competing financial interest.
The data generated that support the findings of this study are available from the corresponding authors upon reasonable request.

■ ACKNOWLEDGMENTS

We wish to acknowledge the helpful guidance of Dr. Tony Durst throughout the course of this work. We also acknowledge the technical assistance of Dr. Mojmír Suchý.

■ REFERENCES

(1) Abrams, D. I. The Therapeutic Effects of Cannabis and Cannabinoids: An Update from the National Academies of Sciences, Engineering and Medicine Report. *Eur. J. Intern. Med.* **2018**, *49*, 7−11.
(2) Hajizadeh, M. Legalizing and Regulating Marijuana in Canada: Review of Potential Economic, Social, and Health Impacts. *Int. J. Heal. Policy Manag.* **2016**, *5*, 453−456.
(3) Rehm, J.; Fischer, B. Cannabis Legalization With Strict Regulation, the Overall Superior Policy Option for Public Health. *Clin. Pharmacol. Ther.* **2015**, *97*, 541−544.
(4) Hall, W.; Weier, M. Assessing the Public Health Impacts of Legalizing Recreational Cannabis Use in the USA. *Clin. Pharmacol. Ther.* **2015**, *97*, 607−615.
(5) Turner, C. E.; Elsohly, M. A.; Boeren, E. G. Constituents of *Cannabis sativa* L. XVII. A Review of the Natural Constituents. *J. Nat. Prod.* **1980**, *43*, 169−234.
(6) Veress, T.; Szanto, J. I.; Leisztner, L. Determination of Cannabinoid Acids by High-Performance Liquid Chromatography of Their Neutral Derivatives Formed by Thermal Decarboxylation: I. Study of the Decarboxylation Process in Open Reactors. *J. Chromatogr. A* **1990**, *520*, 339−347.
(7) Ahmed, S. A.; Ross, S. A.; Slade, D.; Radwan, M. M.; Khan, I. A.; ElSohly, M. A. Minor Oxygenated Cannabinoids from High Potency *Cannabis sativa* L. *Phytochemistry* **2015**, *117*, 194−199.

DOI: 10.1021/acssensors.9b01150
ACS Sens. 2019, 4, 2706−2715

(8) ElSohly, M. A.; Gul, W. Constituents of *Cannabis sativa*. In *Handbook of Cannabis*; Oxford University Press, 2014; pp 3−22.
(9) Kunos, G.; Osei-Hyiaman, D.; Bátkai, S.; Sharkey, K. A.; Makriyannis, A. Should Peripheral CB1 Cannabinoid Receptors Be Selectively Targeted for Therapeutic Gain? *Trends Pharmacol. Sci.* **2009**, *30*, 1−7.
(10) Mechoulam, R.; Peters, M.; Murillo-Rodriguez, E.; Hanuš, L. O. Cannabidiol − Recent Advances. *Chem. Biodivers.* **2007**, *4*, 1678−1692.
(11) Ujváry, I.; Hanuš, L. Human Metabolites of Cannabidiol: A Review on Their Formation, Biological Activity, and Relevance in Therapy. *Cannabis Cannabinoid Res.* **2016**, *1*, 90−101.
(12) Seeman, P. Cannabidiol Is a Partial Agonist at Dopamine D2High Receptors, Predicting Its Antipsychotic Clinical Dose. *Transl. Psychiatry* **2016**, *6*, No. e920.
(13) Weiss, L.; Zeira, M.; Reich, S.; Har-Noy, M.; Mechoulam, R.; Slavin, S.; Gallily, R. Cannabidiol Lowers Incidence of Diabetes in Non-Obese Diabetic Mice. *Autoimmunity* **2006**, *39*, 143−151.
(14) Nissim, R.; Compton, R. G. Absorptive Stripping Voltammetry for Cannabis Detection. *Chem. Cent. J.* **2015**, *9*, 41.
(15) Kintz, P.; Cirimele, V.; Ludes, B. Detection of Cannabis in Oral Fluid (Saliva) and Forehead Wipes (Sweat) from Impaired Drivers. *J. Anal. Toxicol.* **2000**, *24*, 557−561.
(16) Beck, O.; Sandqvist, S.; Dubbelboer, I.; Franck, J. Detection of 9-Tetrahydrocannabinol in Exhaled Breath Collected from Cannabis Users. *J. Anal. Toxicol.* **2011**, *35*, 541−544.
(17) Hartman, R. L.; Huestis, M. A. Cannabis Effects on Driving Skills. *Clin. Chem.* **2013**, *59*, 478−492.
(18) Lau-Cam, C. A.; Pizzitola, V. Simple Field Test for Marijuana. *J. Pharm. Sci.* **1979**, *68*, 976−978.
(19) Mali, B. D.; Parulekar, P. P. Diazotized Dapsone as a Reagent for the Detection of Cannabinoids on Thin-Layer Chromatograpic Plates. *J. Chromatogr. A* **1988**, *457*, 383−386.
(20) dos Santos, N. A.; Souza, L. M.; Domingos, E.; França, H. S.; Lacerda, V.; Beatriz, A.; Vaz, B. G.; Rodrigues, R. R. T.; Carvalho, V. V.; Merlo, B. B.; et al. Evaluating the Selectivity of Colorimetric Test (Fast Blue BB Salt) for the Cannabinoids Identification in Marijuana Street Samples by UV−Vis, TLC, ESI(+)FT-ICR MS and ESI(+)-MS/MS. *Forensic Chem.* **2016**, *1*, 13−21.
(21) Nascimento, I. R.; Costa, H. B.; Souza, L. M.; Soprani, L. C.; Merlo, B. B.; Romão, W. Chemical Identification of Cannabinoids in Street Marijuana Samples Using Electrospray Ionization FT-ICR Mass Spectrometry. *Anal. Methods* **2015**, *7*, 1415−1424.
(22) Watanabe, K.; Yamaki, E.; Yamamoto, I.; Yoshimura, H. A Colorimetric Method for the Determination of Cannabinoids with Fast Blue BB Salt. *Eisei kagaku* **1979**, *25*, 321−326.
(23) Lester, G. E.; Lewers, K. S.; Medina, M. B.; Saftner, R. A. Comparative Analysis of Strawberry Total Phenolics via Fast Blue BB vs. Folin−Ciocalteu: Assay Interference by Ascorbic Acid. *J. Food Compos. Anal.* **2012**, *27*, 102−107.
(24) Torsi, L.; Dodabalapur, A. Organic Thin-Film Transistors as Plastic Analytical Sensors. *Anal. Chem.* **2005**, *77*, 380A−387A.
(25) Melville, O. A.; Lessard, B. H.; Bender, T. P. Phthalocyanine-Based Organic Thin-Film Transistors: A Review of Recent Advances. *ACS Appl. Mater. Interfaces* **2015**, *7*, 13105−13118.
(26) Melville, O. A.; Grant, T. M.; Lessard, B. H. Silicon Phthalocyanines as N-Type Semiconductors in Organic Thin Film Transistors. *J. Mater. Chem. C* **2018**, *6*, 5482−5488.
(27) Sirringhaus, H. Reliability of Organic Field-Effect Transistors. *Adv. Mater.* **2009**, *21*, 3859−3873.
(28) Brixi, S.; Melville, O. A.; Boileau, N. T.; Lessard, B. H. The Influence of Air and Temperature on the Performance of PBDB-T and P3HT in Organic Thin Film Transistors. *J. Mater. Chem. C* **2018**, *6*, 11972−11979.
(29) Liu, J.; Agarwal, M.; Varahramyan, K. Glucose Sensor Based on Organic Thin Film Transistor Using Glucose Oxidase and Conducting Polymer. *Sens. Actuators, B* **2008**, *135*, 195−199.
(30) Zhang, Q.; Subramanian, V. DNA Hybridization Detection with Organic Thin Film Transistors: Toward Fast and Disposable DNA Microarray Chips. *Biosens. Bioelectron.* **2007**, *22*, 3182−3187.
(31) Boileau, N. T.; Melville, O. A.; Mirka, B.; Cranston, R.; Lessard, B. H. P and N Type Copper Phthalocyanines as Effective Semiconductors in Organic Thin-Film Transistor Based DNA Biosensors at Elevated Temperatures. *RSC Adv.* **2019**, *9*, 2133−2142.
(32) Hammock, M. L.; Knopfmacher, O.; Naab, B. D.; Tok, J. B.-H.; Bao, Z. Investigation of Protein Detection Parameters Using Nanofunctionalized Organic Field-Effect Transistors. *ACS Nano* **2013**, *7*, 3970−3980.
(33) Khan, H. U.; Jang, J.; Kim, J.-J.; Knoll, W. Effect of Passivation on the Sensitivity and Stability of Pentacene Transistor Sensors in Aqueous Media. *Biosens. Bioelectron.* **2011**, *26*, 4217−4221.
(34) Huang, W.; Besar, K.; LeCover, R.; Dulloor, P.; Sinha, J.; Martínez Hardigree, J. F.; Pick, C.; Swavola, J.; Everett, A. D.; Frechette, J.; et al. Label-Free Brain Injury Biomarker Detection Based on Highly Sensitive Large Area Organic Thin Film Transistor with Hybrid Coupling Layer. *Chem. Sci* **2014**, *5*, 416−426.
(35) Zhu, Z.-T.; Mason, J. T.; Dieckmann, R.; Malliaras, G. G. Humidity Sensors Based on Pentacene Thin-Film Transistors. *Appl. Phys. Lett.* **2002**, *81*, 4643−4645.
(36) Xie, T.; Xie, G.; Su, Y.; Hongfei, D.; Ye, Z.; Jiang, Y. Ammonia Gas Sensors Based on Poly (3-Hexylthiophene)-Molybdenum Disulfide Film Transistors. *Nanotechnology* **2016**, *27*, No. 065502.
(37) Zhuang, X.; Han, S.; Huai, B.; Shi, W.; Junsheng, Y. Sub-Ppm and High Response Organic Thin-Film Transistor NO2 Sensor Based on Nanofibrillar Structured TIPS-Pentacene. *Sens. Actuators, B* **2019**, *279*, 238−244.
(38) Chaure, N. B.; Cammidge, A. N.; Chambrier, I.; Cook, M. J.; Cain, M. G.; Murphy, C. E.; Pal, C.; Ray, A. K. High-Mobility Solution-Processed Copper Phthalocyanine-Based Organic Field-Effect Transistors. *Sci. Technol. Adv. Mater.* **2011**, *12*, No. 025001.
(39) Nénon, S.; Kanehira, D.; Yoshimoto, N.; Fages, F.; Videlot-Ackermann, C. Shelf-Life Time Test of p- and n-Channel Organic Thin Film Transistors Using Copper Phthalocyanines. *Thin Solid Films* **2010**, *518*, 5593−5598.
(40) Ji, Z.; Wong, K.; Tse, P.; Kwok, R. W.; Lau, W. Copper Phthalocyanine Film Grown by Vacuum Deposition under Magnetic Field. *Thin Solid Films* **2002**, *402*, 79−82.
(41) Hailey, A. K.; Petty, A. J., II; Washbourne, J.; Thorley, K. J.; Parkin, S. R.; Anthony, J. E.; Loo, Y.-L. Understanding the Crystal Packing and Organic Thin-Film Transistor Performance in Isomeric Guest-Host Systems. *Adv. Mater.* **2017**, *29*, No. 1700048.
(42) Eloff, J. Which Extractant Should Be Used for the Screening and Isolation of Antimicrobial Components from Plants? *J. Ethnopharmacol.* **1998**, *60*, 1−8.
(43) Hazekamp, A.; Bastola, K.; Rashidi, H.; Bender, J.; Verpoorte, R. Cannabis Tea Revisited: A Systematic Evaluation of the Cannabinoid Composition of Cannabis Tea. *J. Ethnopharmacol.* **2007**, *113*, 85−90.
(44) Aizpurua-Olaizola, O.; Omar, J.; Navarro, P.; Olivares, M.; Etxebarria, N.; Usobiaga, A. Identification and Quantification of Cannabinoids in *Cannabis sativa* L. Plants by High Performance Liquid Chromatography-Mass Spectrometry. *Anal. Bioanal. Chem.* **2014**, *406*, 7549−7560.
(45) Stolker, A. A. M.; van Schoonhoven, J.; de Vries, A. J.; Bobeldijk-Pastorova, I.; Vaes, W. H. J.; van den Berg, R. Determination of Cannabinoids in Cannabis Products Using Liquid Chromatography−Ion Trap Mass Spectrometry. *J. Chromatogr. A* **2004**, *1058*, 143−151.
(46) Zhang, X.; Chen, Y. A Sandwich Mixed (Phthalocyaninato) (Porphyrinato) Europium Triple-Decker: Balanced-Mobility, Ambipolar Organic Thin-Film Transistor. *Inorg. Chem. Commun.* **2014**, *39*, 79−82.
(47) Kumar, P.; Santhakumar, K.; Shin, P.-K.; Ochiai, S. Improving the Photovoltaic Parameters of Organic Solar Cell Using Soluble Copper Phthalocyanine Nanoparticles as a Buffer Layer. *Jpn. J. Appl. Phys.* **2014**, *53*, No. 01AB06.

DOI: 10.1021/acssensors.9b01150
ACS Sens. 2019, 4, 2706−2715

(48) Margham, J.; McAdam, K.; Forster, M.; Liu, C.; Wright, C.; Mariner, D.; Proctor, C. Chemical Composition of Aerosol from an E-Cigarette: A Quantitative Comparison with Cigarette Smoke. *Chem. Res. Toxicol.* **2016**, *29*, 1662−1678.
(49) Elkington, D.; Cooling, N.; Belcher, W.; Dastoor, P.; Zhou, X. Organic Thin-Film Transistor (OTFT)-Based Sensors. *Electronics* **2014**, *3*, 234−254.

DOI: 10.1021/acssensors.9b01150
ACS Sens. 2019, 4, 2706−2715